Ultrasound in Med. & Biol., Vol. 48, No. 6, pp. 1095–1109, 2022

0301-5629/$ - see front matter

https://doi.org/10.1016/j.ultrasmedbio.2022.02.007

● *Original Contribution*

CHARACTERIZATION OF ACOUSTIC, CAVITATION, AND THERMAL PROPERTIES OF POLY(VINYL ALCOHOL) HYDROGELS FOR USE AS THERAPEUTIC ULTRASOUND TISSUE MIMICS

Lisa Braunstein,* Sarah C. Brüningk,*,†,‡ Ian Rivens,* John Civale,* and Gail ter Haar*

* Joint Department of Physics at The Institute of Cancer Research and The Royal Marsden NHS Foundation Trust, London, United Kingdom; † Machine Learning & Computational Biology Lab, Department of Biosystems Science and Engineering, ETH Zurich, Basel, Switzerland; and ‡ SIB Swiss Institute of Bioinformatics, Lausanne, Switzerland

(*Received* 23 *August* 2021; *revised* 19 *January* 2022; *in final form* 6 *February* 2022)

Abstract—The thermal and mechanical effects induced in tissue by ultrasound can be exploited for therapeutic applications. Tissue-mimicking materials (TMMs), reflecting different soft tissue properties, are required for experimental evaluation of therapeutic potential. In the study described here, poly(vinyl alcohol) (PVA) hydrogels were characterized. Hydrogels prepared using different concentrations (5%–20% w/w) and molecular weights of PVA ± cellulose scatterers (2.5%–10% w/w) were characterized acoustically (sound speed, attenuation) as a function of temperature (25°C–45°C), thermally (thermal conductivity, specific heat capacity) and in terms of their cavitation thresholds. Results were compared with measurements in fresh sheep tissue (kidney, liver, spleen). Sound speed depended most strongly on PVA concentration, and attenuation, on cellulose content. For the range of formulations investigated, the PVA gel acoustic properties (sound speed: 1532 ± 17 to 1590 ± 9 m/s, attenuation coefficient: 0.08 ± 0.01 to 0.37 ± 0.02 dB/cm) fell within those measured in fresh tissue. Cavitation thresholds for 10% PVA hydrogels (50% occurrence: 4.1–5.4 MPa, 75% occurrence: 5.4–8.2 MPa) decreased with increasing cellulose content. In summary, PVA cellulose composite hydrogels may be suitable mimics of acoustic, cavitation and thermal properties of soft tissue for a number of therapeutic ultrasound applications. (E-mail: lisa.braunstein@icr.ac.uk)

Key Words: **Focused ultrasound, High-intensity focused ultrasound, Therapeutic ultrasound, Tissue mimic, Poly (vinyl alcohol), Cavitation thresholds, Acoustic properties, Thermal properties, Phantom material.**

INTRODUCTION

Ultrasound (US) not only is used for diagnostic imaging, but is also increasingly being exploited for its potential in therapy (Miller et al. 2013; Yang et al. 2019). When an ultrasonic wave travels through tissue, it can invoke thermal and/or mechanical effects. Thermal effects result from the loss of ultrasound energy from absorption as a beam travels through tissue. Mechanical effects can arise from shear stresses caused by the incident acoustic pressures and from acoustic cavitation, the formation and/or activity of microscopic vapor-filled bubbles (Coakley and Nyborg 1978; Apfel 1981). Two types of cavitation are distinguished: non-inertial, in which bubbles in tissue oscillate in resonance with the incident acoustic beam, and inertial, in which the bubbles grow rapidly and collapse violently (Hill 2004). Both thermal and mechanical effects of US can be harnessed for a number of therapeutic applications ranging from hyperthermic therapy, in which tissue temperature is increased to 40°C–45°C for minutes to ~1 h (Zhu et al. 2019); and thermal ablation, which uses temperatures >56°C to induce coagulative necrosis (ter Haar 2007), to histotripsy (Roberts 2014; Vlaisavljevich et al. 2016), sonophoresis, sonoporation (Hu et al. 2013), lithotripsy (Miller and Lingeman 2007; Roberts 2014) and US-enhanced drug delivery (Unger et al. 2002), which exploit mechanical US effects. Materials that mimic the acoustic and thermal parameters of tissue are valuable for laboratory studies, for example, in validating simulated temperature and pressure distributions and in

Address correspondence to: Lisa Braunstein, The Institute of Cancer Research, 15 Cotswold Road, SM25NG, Sutton, UK. E-mail: lisa.braunstein@icr.ac.uk

determining optimal acoustic beam characteristics for the anticipated application (Culjat et al. 2010; Cook et al. 2011; Cabrelli et al. 2017). These preparations are referred to as tissue-mimicking materials (TMMs). Importantly, a TMM's acoustic characteristics, such as sound speed, attenuation and acoustic impedance, as well as its cavitation threshold and thermal properties, specific heat capacity and thermal conductivity should reflect the range of those found in human soft tissues such as brain, liver, kidney, spleen and muscle. Ideally, TMMs and their production should be low-cost, reproducible and safe.

As biological soft tissue has a high water content, hydrogels formed from cross-linked, water-absorbent polymers have previously been suggested as TMMs, as their acoustic properties resemble those of soft tissue (Culjat et al. 2010). Commonly used hydrogels are formed from natural gelling agents, for example, agar, agarose (Cook et al. 2011; Cafarelli et al. 2017) and gelatine (Culjat et al. 2010), or synthetic polymers such as poly(vinyl alcohol) (PVA) (Prokop et al. 2003; Hou et al. 2015) and poly(acrylamide) (PAA) (Howard et al. 2003; Cafarelli et al. 2017). Table 1 provides an overview of the relevant advantages and drawbacks for a selection of TMMs produced from both natural and synthetic polymers. Although hydrogels from most of these polymers have been characterized in terms of sound speed and attenuation coefficients (Zell et al. 2007; Cook et al. 2011; Cafarelli et al. 2017), there is little information regarding their thermal properties and cavitation thresholds.

From this range of potential TMM candidate materials, PVA hydrogels have recently been suggested as being suitable for focused ultrasound (FUS) applications, which exploit thermal effects (Crivoi et al. 2007; ter Haar and Coussios 2007; Brüningk et al., 2019), and have incorporated thermochromic dye to monitor heating patterns (Ambrogio et al. 2020). PVA is an cheap, biocompatible synthetic polymer that forms hydrogels from aqueous solutions. The hydrogel's mechanical strength varies with the molecular weight of the PVA used and the method by which they are crosslinked. Crosslinking can be achieved physically (using freeze-thaw cycles) (Hassan and Peppas 2000), by irradiation (*e.g.,* using γ-irradiation, at a dose of 30 kGy with a dose rate of 0.76 kGy/h [Yang et al. 2007]) or by chemical means (*e.g.,* using blocked isocyanate prepolymer [Lee et al. 2010] or formaldehyde [Yang et al. 2012]). A number of previous studies have investigated the mechanical and acoustic properties of different PVA hydrogel formulations (Prokop et al. 2003; Hou et al. 2015; Silver and Shah 2016). The acoustic and thermal properties of PVA hydrogels from different recipes generally lie within the range of those of human soft tissue (Zell et al. 2007; Culjat et al. 2010). It has been reported that the acoustic attenuation of PVA hydrogels can be tuned by addition of scatterers such as glass beads (Cafarelli et al. 2017), graphite powder (Culjat et al. 2010), talcum powder (Taghizadeh et al. 2018) and cellulose (Brüningk et al., 2019). Additionally, sound speed has been adjusted by addition of 1-propanol (Holt and Roy 2001). Despite these promising data, a thorough analysis of acoustic and thermal property dependence on different gel formulations is missing. Importantly, the cavitation threshold has also not previously been quantified for these TMMs. A comprehensive catalogue of all these properties would render PVA hydrogels a more useful tool for the therapeutic US community.

Table 1. Overview of the advantages and disadvantages of various tissue-mimicking materials

Material	Advantages	Disadvantages	References
Agar and agarose	• Ease of production • Transparent	• Acoustic properties strongly dependent on method of production and composition of mixture • Limited lifetime • Expensive (especially agarose)	Culjat et al. 2010; Cafarelli et al. 2017
Gelatine	• Inexpensive • Stable over time	• Low thermal stability	Culjat et al. 2010; Cook et al. 2011
Poly(acrylamide)	• Transparent gel • Bovine serum albumin can be added to visualize coagulation	• Neurotoxin • Low attenuation coefficient	Howard et al. 2003; Prokop et al. 2003; Lafon et al. 2005; Zell et al. 2007
Poly(vinyl alcohol)	• Inexpensive • Transparent gels possible • Long lifetime	• Crosslinking process needed • Transparent gels are weaker • Time-consuming production	Maolin et al. 2002; Crivoi et al. 2007; Yang et al. 2007; Culjat et al. 2010; Hou et al. 2015

This study aimed to map the dependence of acoustic (sound speed, acoustic attenuation, cavitation thresholds) and thermal (thermal conductivity, specific heat capacity) properties of PVA hydrogels as a function of PVA molecular weight and PVA and cellulose content in the temperature range 20°C−45°C. Furthermore, the acoustic and thermal properties obtained were compared with those of fresh ex vivo sheep kidney, liver and spleen tissue measured at room temperature.

METHODS

Sample preparation

Poly(vinyl alcohol) cryogels were prepared as described previously (Brüningk et al., 2019) from PVA granules, degassed, deionized water (dissolved oxygen concentration: 1.5 ± 0.3 mg/L, 18.2Ω), and, optionally, cellulose powder (1001318450, Type 20, 20 μm, Sigma Aldrich, Dorset, UK) using the different formulations described in Table 2. Ten percent PVA cryogels were prepared from PVAs of three different molecular weights: 85,000-124,000 g/mol (PVA_{medium}, No. 1002846189, Sigma Aldrich), 146,000−186,000 g/mol (PVA_{high}, No. 1002817065, Sigma Aldrich) and 31,000−50,000 g/mol (PVA_{low}, No. 1002778863, Sigma Aldrich). PVA concentration ranged from 5% to 20% (w/w), with optional 0 to 10% (w/w) cellulose. All gel solutions were crosslinked in a custom-built perspex mould (12 × 14 cm, depth 0.6 or 1.2 cm depending on application Brüningk et al., 2019) using three cycles of 5 h freezing (at −20°C) and 19 h thawing to room temperature (RT) (20°C) in a timer-controlled freezer. The gel sheet was cut into 5.5 cm-diameter cylinders, which were subsequently sterilized by immersion in 70% ethanol for 1 h to allow their potential use as a substrate for exposure of cell cultures to FUS under aseptic conditions (Brüningk et al., 2019). These disks were stored in deionized water in a fridge for 1−3 d prior to characterization to allow the samples to equilibrate their water content. They were then removed from the fridge and allowed to reach room temperature (RT, 20 ± 1°C) for 1 h prior to characterization measurements. At least three independent batches of samples were produced for each formulation tested. Only freshly prepared samples were analyzed.

Table 2. Composition of PVA (cellulose) gel formulations produced from PVA of molecular weight 85,000−124,000 g/mol*

Formulation	Water (mL)	PVA (g)	Cellulose (g)
5% PVA 0% cellulose	150	7.9	0
5% PVA 5% cellulose	150	7.9	7.9
10% PVA 0% cellulose†	150	16.7	0
10% PVA 2.5% cellulose	150	16.7	3.8
10% PVA 5% cellulose	150	16.7	7.9
10% PVA 10% cellulose	150	16.7	16.7
15% PVA 0% cellulose	150	26.5	0
15% PVA 5% cellulose	150	26.5	7.9
20% PVA 0% cellulose	150	37.5	0
20% PVA 5% cellulose	150	37.5	7.9

PVA = poly(vinyl alcohol).

* The cellulose was added in the same amount as calculated for pure PVA hydrogels to keep the water-to-PVA ratio consistent.

† Gels of 10% PVA 0% cellulose were also produced of PVA of molecular weight of 31,000−50,000 g/mol and 146,000−186,000 g/mol.

Fresh, ex vivo tissue (liver, two kidneys and spleen) was acquired from three sheep and acoustically characterized. Additionally, three samples of sheep liver and six of sheep kidneys were acquired from a local butcher and were thermally characterized. Kidney samples were measured whole and with the sides cut, as illustrated in Figure 1 (A, B). Liver and spleen were cut as illustrated in Figure 1 (C, D).

Acoustic characterization

Acoustic attenuation coefficient (a) and sound speed were measured using the finite amplitude insertion-substitution (FAIS) method, with the experimental setup described by Retat (2011) (see Fig. 2). It consisted of two matched, weakly focused, ultrasonic broadband transducers (center frequency = 2 MHz, frequency range: 1.5−3.5 MHz, 2.5 cm diameter, 10 cm diameter, Imasonic SAS, Besancon, France), a sample holder (with plane parallel windows of 23 μm PMX980, HiFi Industrial film, Stevenage, UK) mounted on a motorized gantry, consisting of a motion controller (ViX250IM Parker

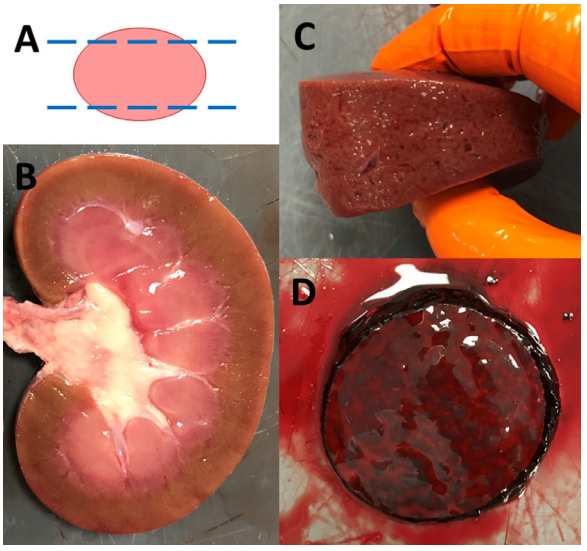

Fig. 1. (A) Schematic of a kidney viewed end on, illustrating how the outer surfaces were cut to create a parallel-sided flat sample as shown in (B) and (C) for liver and (D) for spleen cut into 5.5-cm-diameter cylindrical samples for characterization.

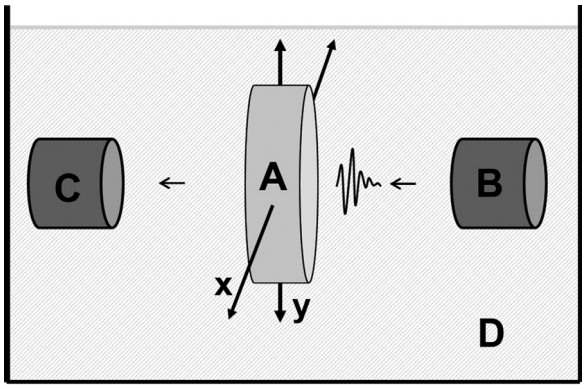

Fig. 2. Schematic diagram of the experimental arrangement used for acoustic characterization using the finite amplitude insertion-substitution method. The sample holder (A) is mounted on an automated gantry, placed equidistant between the two 2 MHz transducers (B: transmitter, C: receiver) and can be moved to different lateral measurement positions in the x- and y-directions by a motion controller together with position encoders. The sample holder can also be moved out of the pulse path to allow reference measurements in water. The system is placed in a temperature-controlled tank of degassed water (D).

Vix, IL, USA), axes (Unislide linear slides, LG Motion, Basingstoke, UK) and position encoders (LM13 Incremental Magnetic Encoder, RLS, Lubjiana, Slovenia). A thermocouple (TJ36-CASS-010-U-12, Omega Engineering Ltd, Manchester, UK) and thermocouple reader (NI-USB-TC01, National Instruments, Austin, TX, USA) were used to measure the water bath temperature. This was controlled by simultaneously using a heater (GD100, Grant Instruments Ltd, Cambridge, UK) and a chiller (HC-100A, Hailea, Guandong, China). As in previous work, for each measurement two 0.6 cm thick cylindrical PVA samples were sandwiched in the sample holder (Brüningk et al., 2019).

Pulsed acoustic signals (time between pulses: 10 ms) were generated by a pulse generator (DPR300, JSR Ultrasonics, NY, USA) with approximate peak pressures of 0.017 MPa (negative) and 0.015 MPa (positive) at a distance of 10 cm from the transmitter, coinciding with the position of the sample holder during acoustic characterization measurements. To increase the signal-to noise-ratio, 200 consecutive waves were averaged by an oscilloscope (5444D, PicoScope, Cambs, UK). These were measured over a grid consisting of 11 × 11 points at 2 mm separation in a plane orthogonal to the beam direction. The edges of the cylindrical samples were avoided to prevent partial volume effects (in the form of signal from both the water bath and the sample holder).

The sound speed of the reference medium (degassed water) was estimated using the known temperature dependence for water from the water bath temperature measured using a thermocouple. Sample thickness and speed of sound were estimated from the pulse-echo times (arising from reflections from the front and back windows) and the difference in the time of flight of the transmitted pulse after transit through the sample or the reference medium alone (Retat 2011). The attenuation coefficient (α) and frequency dependence of attenuation (N) were estimated using the FAIS method as described in Hill (2004, Ch. 4). The mean values and standard deviations for all measured values were calculated from 121 data points meeting the following minimum quality requirements: (i) distinct echoes from both the sample's front and back surfaces were detected, (ii) the measured sample thickness was within 10% of the average caliper-measured thickness of the physical sample and (iii) no air bubbles were present (either visible or causing clear circular measurement artefacts).

Measurements were performed for all PVA samples at increasing temperatures (20°C−45°C in 5°C steps). Samples were left to equilibrate to each target temperature in a temperature-controlled water bath for 20 min prior to measurement.

The kidney, liver and spleen samples were contained in the sample holder, making sure that the membranes (with a separation of 2 cm) were tight but did not overly compress the sample. Measurements were performed at RT for each sample.

Cavitation threshold measurements

To establish inertial and non-inertial cavitation thresholds, the occurrence of both half-harmonic signals (characteristic of stable bubble oscillation) and broadband signals (indicative of collapsing bubbles) were analyzed. A 17.5 mm diameter, 64 mm focal length and 63.2 mm radius of curvature (Y107, Sonic Concepts, Seattle, WA, USA) cavitation sensor, located in the central aperture of a 1.66 MHz, 64 mm focal length, 63 mm diameter HIFU transducer (H148-MR, Sonic Concepts) was mounted on a computer-controlled 3-D positioning system. A waveform generator (33250A, Agilent, Santa Clara, USA) provided an input voltage, which was amplified (A300, 55 dB, E&I Rochester, NY, USA) to drive the HIFU transducer. The HIFU transducer's focal peak negative pressure (PNP) was measured using a calibrated hydrophone (AG-2020 Preamplifier, Onda, Sunnyvale, CA, USA) in deionized degassed water under free field conditions, over a range of drive voltages (corresponding to a PNP range of 1.76 to 9.64 MPa) with 10% uncertainty. The passive cavitation detection (PCD) sensor (bandwidth = 1−20 MHz) was connected via a 1.7 MHz notch filter (F5181, Allen Avionics, Chicago, IL, USA, used to remove the fundamental of the drive signal) and a 20 dB pre-amplifier (P0.1-30/20VD, Advanced Receiver Research Ar^2, Burlington, MA, USA) to a data acquisition card (M2i.3024, Spectrum,

Stuttgart, Germany) installed in a SuperMicro computer (LGA 1150, SuperMicro, San Jose, CA, USA). Both the HIFU drive voltage/1000 and the detected cavitation signal were logged at a rate of 50 MHz. Measurements were performed in a tank filled with deionized degassed water (0.1−0.7 mg/L, 20°C) with an acoustic absorber on its base to reduce reflections. To provide a constant level of degassing and temperature, the water was circulated through a chilling system (HC-100A, Hailea, Guangdong, China) with a liquicell (2.5 × 8 Liqui-Cel Membrane Contactor, Membrana, Charlotte, NC, USA) connected to a vacuum line (27 in. Hg). The PVA sample size for cavitation threshold measurements was 5 × 10 × 1.2 cm to ensure that the focal point (1.6 × 1.4 × 12.4 mm) of the transducer lie entirely within the sample. Samples were pinned to a thin membrane (23 μm PMX980, HiFi Industrial film, Stevenage, UK) in the focal plane of the HIFU transducer, with needles placed at the unexposed sample edges. Exposures consisted of ten 10 ms pulses, at a pulse repetition frequency of 1 Hz in each position, at a peak negative pressure (PNP) of 1.8 to 9.6 MPa. Exposures were placed 1 cm apart to avoid any overlap of the focused beam between positions. To ensure reproducible measurements and to make sure there were no spurious signals from the water, baseline measurements were performed in degassed water. The recorded cavitation data were analyzed to reveal the half-harmonic (0.8 MHz) and broadband (0.1-10 MHz) signals, the latter after software filtering to remove all $n/6$ harmonics of the drive signal below the Nyquist limit, where n is an integer.

Inertial cavitation threshold levels are quantified as the PNP at which 25%, 50% and 75% of the exposures (10 in each position, 2 positions per gel, *i.e.,* 20 exposures in total) resulted in broadband signals above baseline noise. Here, "baseline noise" is defined as the average off-time signal. Signals exceeding this baseline by more than a factor of 5 were considered to be emissions caused by inertial cavitation activity. The measurement was performed in five independently prepared gels for each formulation.

The current experimental setup did not allow the measurement of cavitation thresholds in tissue.

Thermal characterization

Material density, required for thermal characterization, was measured using Archimedes' principle. For thermal characterization (specific heat capacity and thermal conductivity), a HotDisk system (TPS 2500 S, Hot Disk, Goeteborg, Sweden) was used according to the manufacturer's protocol, detailing the transient plane source (TPS) method (Gustavsson et al. 1994). A two-sided TPS sensor was sandwiched between two 0.6 cm PVA gel disks, and three separate 160 s measurements were acquired using an output power of 128.5 mW. A 10 min cooling period between measurements ensured that the sensor and sample returned to RT.

Statistical analysis

Mean values and standard deviations were calculated using data from at least three independently produced samples by first averaging over intra-batch and then inter-batch repeat measurements. Where applicable, the data were checked for normal distribution with the one-sample Kolmogorov-Smirnov test, using the MATLAB (version R2019a) function kstest. For normally distributed data, p values were calculated using the anova1 function in MATLAB; the Kruskal-Wallis test with the function kruskalwallis was used otherwise. We note that given the small number of samples, normality testing may be limited; however, the choice of test (*i.e.,* either analysis of variance or Kruskal-Wallis) did not change the results in terms of the significance of the findings presented. Correlation of data points as a function of temperature, PVA or cellulose concentration was assessed by Pearson correlation coefficients (ρ) with relevant p values obtained from the averaged values using the MATLAB function corr. Any p values <0.05 were scored as significant. The MATLAB curve fitting toolbox was used to fit a linear function for acoustic properties to describe the observed behavior with the simplest approach. The selected fit function was assessed using the coefficients of determination R^2. We consider fits with $R^2 > 0.85$ appropriate. Following Maxwell et al. (2013), we fitted sigmoid functions $F(x) = -c/\left(1 + (x/b)^a\right) + c$ to cavitation event probabilities as function of PNP.

RESULTS

Gel formulation

The molecular weight and overall concentration of PVA affected the water solubility, viscosity of the PVA solution obtained and transparency and thermal stability of the crosslinked gels (see Fig. 3): PVA_{low} took ~50 min to dissolve, whereas PVA_{medium} took ~60 min

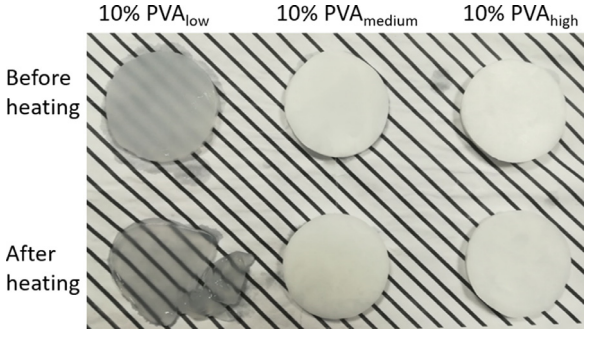

Fig. 3. Ten percent poly(vinyl alcohol) samples of different molecular weight before and after being heated to 45°C.

and PVA_{high} 80−90 min. Aqueous solutions involving PVA_{high} or PVA_{medium} with ≥20% PVA were very viscous, and bubbles were easily trapped in the gels formed. Gels formed using 10% PVA_{low} or ≤5% PVA_{medium} solutions were very soft, tore easily when touched and melted upon heating to 45°C. PVA_{medium} was therefore chosen for further characterization of the influence of the gel formulation. The 10%−15% PVA_{medium} gels provided a compromise between mechanical/thermal stability and viscosity of the PVA solution.

Figure 4 illustrates the acoustic properties of 10% PVA gels of different molecular weight at 20°C. Over the temperature range studied, these were comparable and there were no statistically significant differences (sound speed of 1556−1566 m/s, p = 0.10, attenuation coefficient = 0.08−0.09 dB/cm, p = 0.86, and N = 1.43−1.45, p = 0.85). The thermal properties of PVA gels of varying molecular weight did not differ significantly (thermal conductivity: 0.57−0.6 MJ/m·K, p = 0.20; specific heat capacity: 2.99−3.06 MJ/m^3·K, p = 0.73).

Acoustic properties

As illustrated in Figure 5 (A, B), sound speed and attenuation coefficient both increased linearly with PVA concentration, whereas the exponent of the attenuation frequency dependence N remained constant within the range of measurement uncertainties (Fig. 5C).

The addition of cellulose as scatterer significantly changed neither the sound speed (p = 0.2) nor the frequency dependence (p = 0.22) of the attenuation coefficient in 10% PVA_{medium} gels (at RT) (Fig. 5D, 5F). However, the attenuation coefficient increased linearly with the addition of cellulose (Fig. 5H). The rate of this increase (slope: 0.028 ± 0.012 dB/cm·MHz, R^2 = 0.98) was high compared with the linear increase as a function of PVA concentration (slope: 0.005 ± 0.003 dB/cm·MHz, R^2 = 0.95) in Figure 5B. As depicted in Figure 5 (G, H) for 10% PVA_{medium}, sound speed increased (slope: 1.3 ± 0.9, R^2 = 0.92, p = 0.914, ρ = 0.01), whereas the attenuation coefficient decreased, with temperature (slope: −0.001 ± 0.0003, R^2 = 0.92, ρ = −0.961, p = 0.002). The frequency dependence did not significantly change as a function of either temperature (ρ = 0. 377, p = 0.46), PVA (ρ = 0.023, p = 0.98) or cellulose concentration (ρ = −0.78, p = 0.22).

Cavitation thresholds of PVA

We did not detect any subharmonic that was not associated with broadband emission in our experiments.

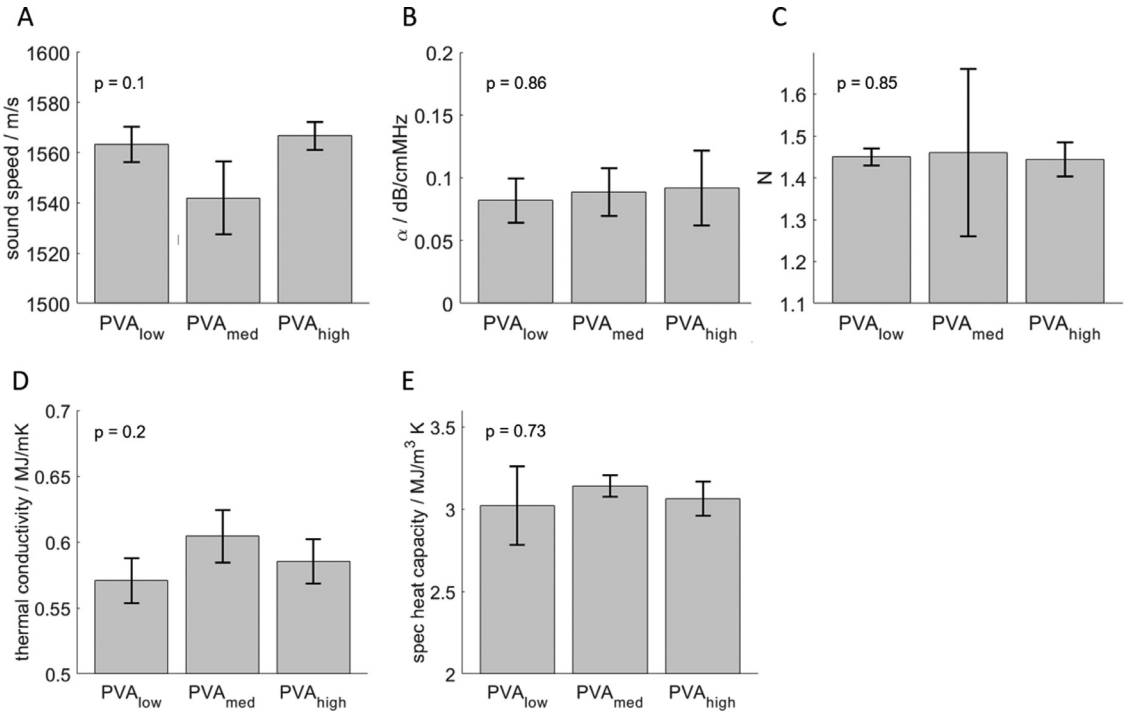

Fig. 4. (A) Sound speed, (B) attenuation coefficient (a), (C) frequency dependence factor (N), (D) thermal conductivity and (E) specific heat capacity plotted as functions of different-molecular-weight 10% poly(vinyl alcohol) (PVA) (PVA_{low}: 31,000−50,000 g/mol, PVA_{medium}: 85,000−124,000 g/mol, and PVA_{high}: 146,000−186,000 g/mol). The mean and standard error of the mean from three independent measurements are shown. p Values were calculated using the analysis of variance or Kruskal-Wallis test; a significance threshold of 0.05 was assumed.

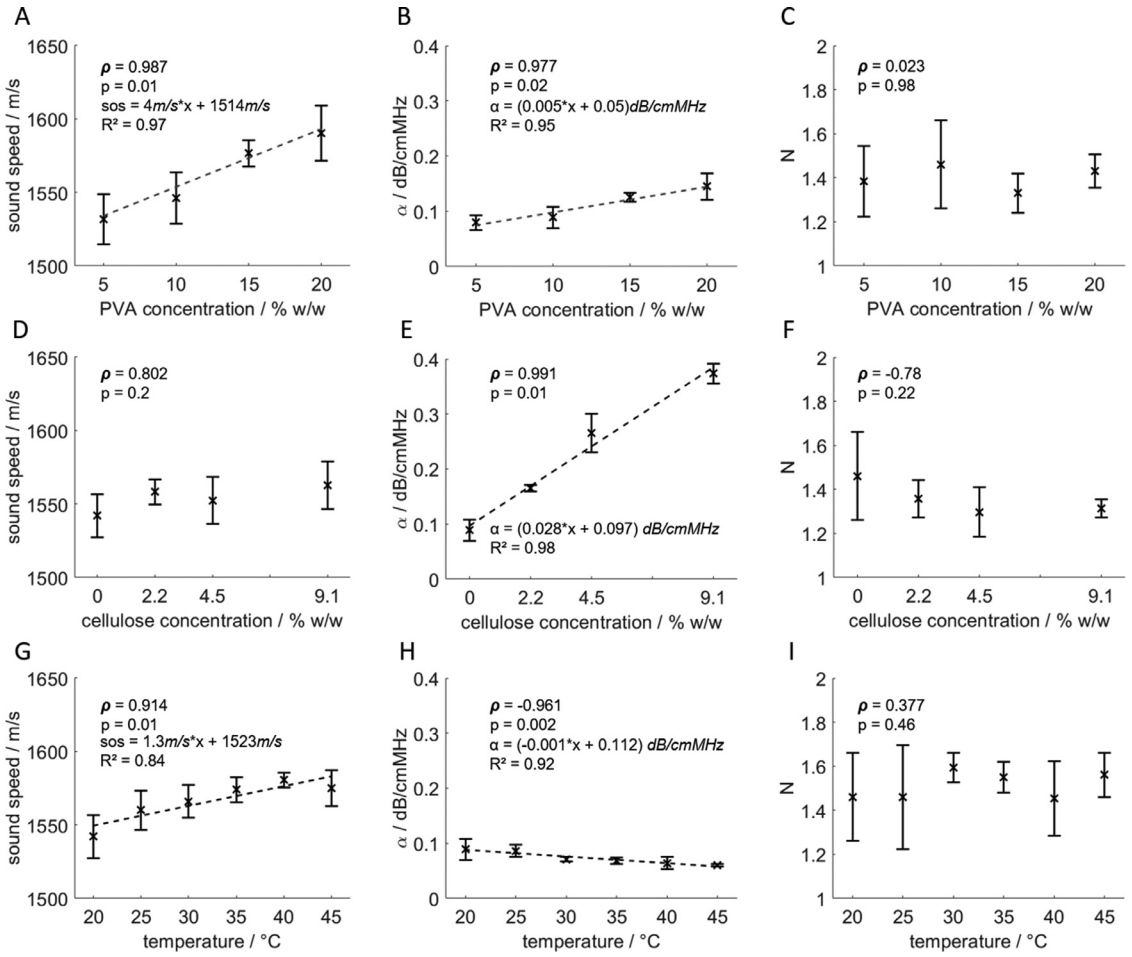

Fig. 5. (A) Sound speed, (B) attenuation coefficient (a) and (C) frequency dependence factor of poly(vinyl alcohol) (PVA) samples (no added cellulose) as a function of PVA concentration at room temperature (RT). (D) Sound speed, (E) attenuation coefficient and (F) frequency dependence factor (N) of 10% PVA samples for different concentrations of cellulose at RT. (G) Sound speed (slope: 1.3 ± 0.9, R^2 = 0.84, ρ = 0.914, p = 0.01). (H) Attenuation coefficient (slope: −0.001 ± 0.0003, R^2 = 0.92, ρ = −0.961, p = 0.002). (I) Frequency dependence factor as a function of temperature for 10% PVA (no cellulose). Mean values with standard error of the mean from three independent measurements are shown, together with Pearson correlation coefficients (ρ) and corresponding p values. Where applicable, linear fits to the mean values with relevant coefficients of determination (R^2) are shown.

Hence all following results refer to inertial cavitation events only. The fraction of n = 20 exposures, which led to cavitation events, is illustrated in Figure 6 as a function of PNP. In more than 20% of exposures it was observed that inertial cavitation could not be generated in degassed water (≤0.4 mg/L dissolved oxygen) in the PNP range 1.8 to 9.6 MPa. Within PVA hydrogels, a sigmoidal trend of the fraction of cavitation events as a function of PNP was observed. Table 3 summarizes the results obtained for three different PVA gel formulations in terms of fit parameters and calculated 25%, 50% and 75% cavitation thresholds. With increasing numbers of cellulose scatterers, the inflection point of the sigmoid curve shifted to lower PNPs, and the slope increased.

Thermal properties

Gel density did not differ significantly between samples, and was independent of PVA concentration (ρ = −0.464, p = 0.54) and cellulose content (ρ = 0.251, p = 0.11) (Fig. 7C, 7F). As illustrated in Figure 7A, thermal conductivity decreased with PVA concentration in samples prepared without cellulose; however, Pearson correlation coefficients were not significant (ρ = −0.923, p = 0.08). The specific heat capacity (ρ = 0.815, p = 0.19) remained fairly constant in the range 10%−20% PVA_{medium} with a drop for 5% PVA_{medium} gels (Fig. 7B). Thermal properties were not influenced (thermal conductivity: ρ = −0.008, p = 0.99; specific heat capacity ρ = −0.811, p = 0.19) by addition of 5% cellulose (Fig. 7D, 7E).

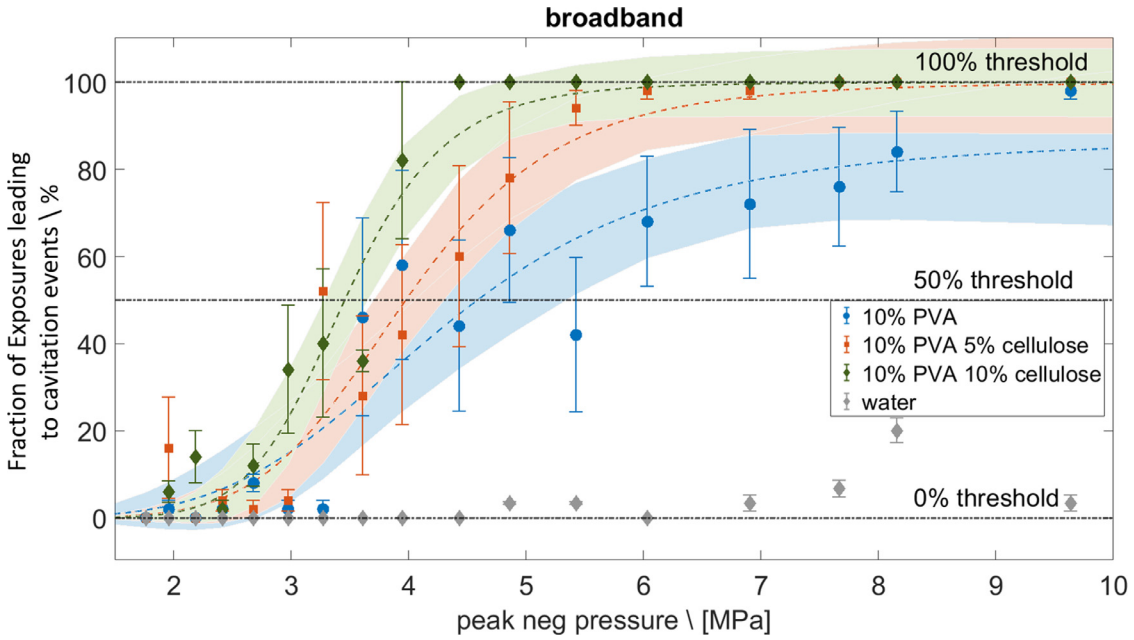

Fig. 6. Percentages of exposures yielding above noise broadband signal, representing signals from collapsing bubbles in 10% poly(vinyl alcohol) (PVA) gels with cellulose concentration ranging from 0% to 10%. Mean values and standard errors of the mean of five independent measurements are shown with sigmoidal fits to the mean values (*dashed lines*) and with corresponding 95% confidence bounds (bands). The 25%, 50% and 75% cavitation thresholds are represented by *horizontal dashed-dotted lines*. The relevant parameterizations are given in Table 3.

Characterization of sheep tissue

The sound speed of the three tissues measured ranged from 1545 ± 8 to 1607 ± 2 m/s with attenuation coefficients of 0.38 ± 0.23 dB/cm·MHz for kidney, 0.53 ± 0.14 dB/cm·MHz for liver and 0.4 ± 0.07 dB/cm·MHz for spleen (Fig. 8A–C) for RT measurements. The splenic thermal properties were not measured because of limited sample availability. The thermal conductivity and specific heat capacity of sheep kidney (0.51 ± 0.01 W/m·K, 3.73 ± 0.61 MJ/m^3·K) and liver (0.49 ± 0.07 W/m·K, 3.07 ± 0.77 MJ/m^3·K) did not differ significantly (Fig. 8D, 8E). The sound speed and the frequency dependence parameters for sheep tissue were within the range measured for PVA hydrogels. The attenuation coefficient of 10% PVA with 10% cellulose was in the range of those for sheep kidney and spleen, whereas sheep liver had a higher attenuation coefficient than any PVA gels investigated here. The thermal conductivity

Table 3. Parameters for sigmoid fits to the function $f(x) = -c/\left(1 + (x/b)^a\right) + c +$ c with a being Hill's slope (%/MPa), b the inflection point (MPa) and c the upper bound (%)*

	10 % PVA	10% PVA 5% cellulose	10% PVA 10% cellulose
a	4.4 ± 2.9	6.1 ± 2.7	8.1 ± 3.2
b	4.3 ± 0.9	4 ± 0.4	3.5 ± 0.1
c	87 ± 23	100 ± 12	100 ± 8
R^2	0.89	0.95	0.96
25% cavitation threshold (MPa)			
Mean	3.5	3.3	3.2
95% CI	3.2–3.9	2.9 3.6	2.8–3.2
50% cavitation threshold (MPa)			
Mean	4.6	4	3.5
95% CI	4.1–5.4	3.7–4.3	3.3–3.6
75% cavitation threshold (MPa)			
Mean	6.5	4.8	4
95% CI	5.4–8.2	4.4–5.4	3.8–4.3

CI = confidence interval; PVA = poly(vinyl alcohol).

* All parameters are reported as median values with 95% confidence intervals together with coefficients of determination, R^2. On the basis of the fits, peak negative pressures yielding 25%, 50% and 75% probability for cavitation were calculated (referred to as "% cavitation thresholds"), and are given with 95% confidence intervals.

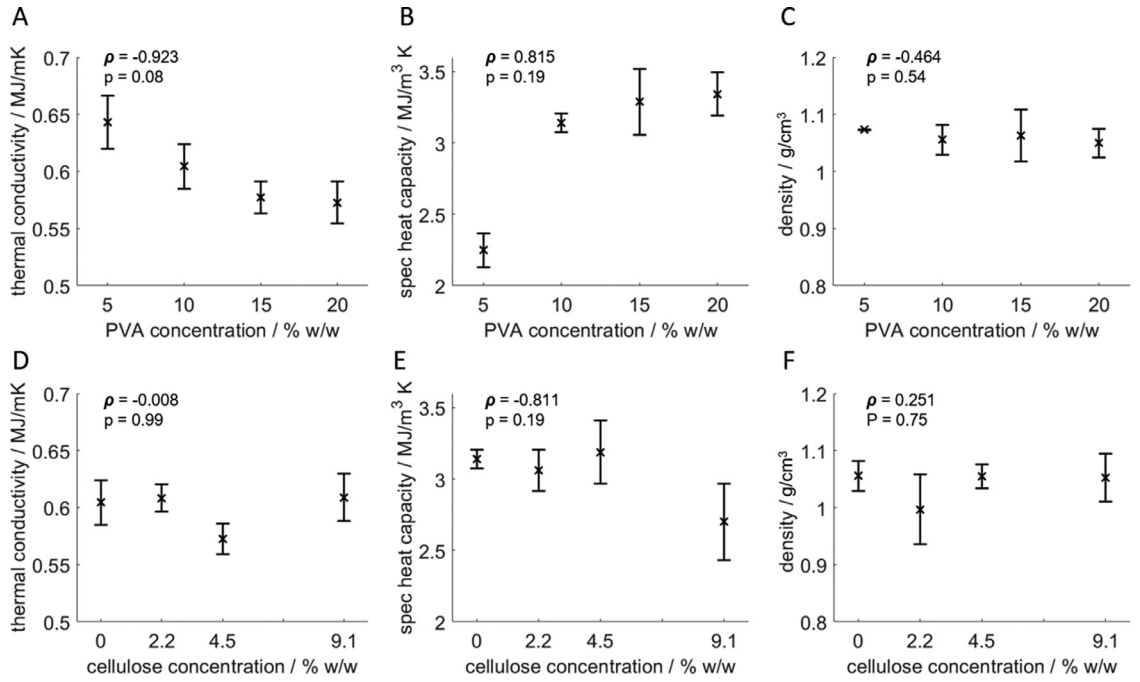

Fig. 7. (A) Thermal conductivity, (B) specific heat capacity and (C) density of poly(vinyl alcohol) (PVA) gels (no added cellulose) as a function of PVA concentration at room temperature. (D) Thermal conductivity, (E) specific heat capacity and (F) density of 10% PVA gels as a function of cellulose concentration at room temperature. Mean values and standard errors of the mean from three independent measurements are given with Pearson correlation coefficients (ρ) and corresponding p values.

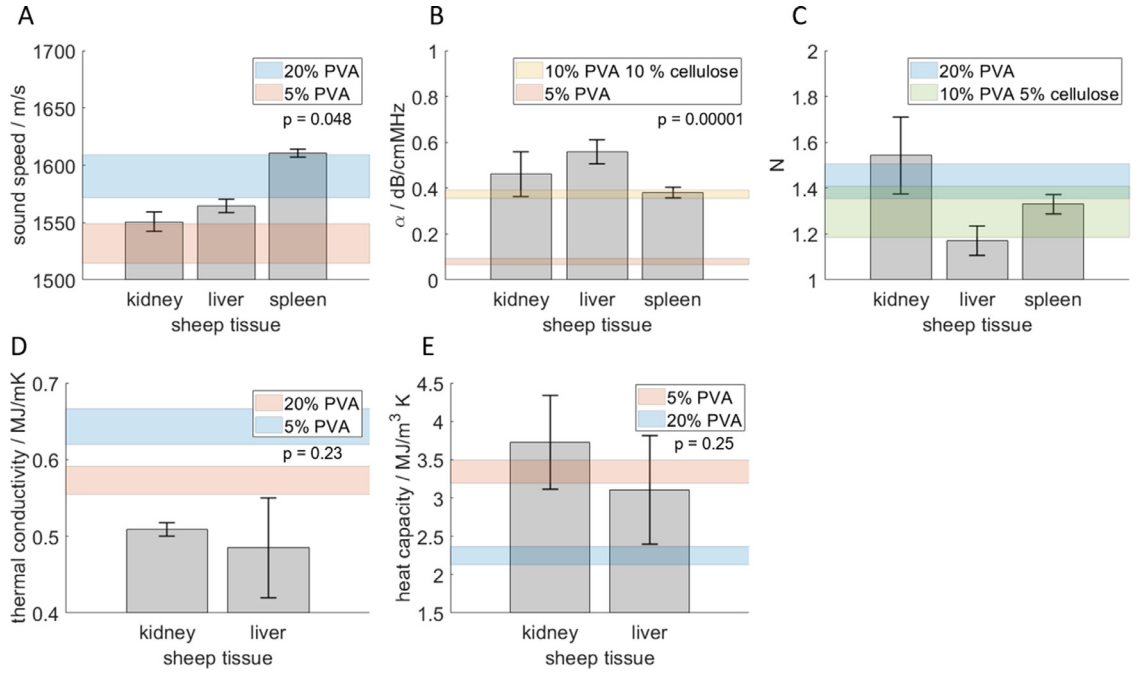

Fig. 8. (A) Sound speed, (B) attenuation coefficient (a) and (C) frequency dependence factor (N) of sheep kidney, liver and spleen tissue at room temperature (RT). (D) Specific heat capacity and (E) thermal conductivity for sheep kidney and liver tissue at RT. Minimum and maximum values measured for PVA gels (with or without cellulose) are shown for comparison. Tissue and PVA data are mean values and standard errors of the mean from three independent measurements. p Values were calculated using the analysis of variance or Kruskal-Wallis test.

values of sheep kidney and liver were lower than the minimum values measured for PVA gels. However, the specific heat capacity of measured tissue was within the range measured for PVA gels.

DISCUSSION

This study provides comprehensive characterization of acoustic, cavitation and thermal properties of PVA (cellulose) hydrogels to determine their suitability as mimics for use in FUS experiments. A range of hydrogel formulations, comprising varying concentrations of PVA and cellulose, and three different PVA molecular weights, were analyzed. Fresh, ex vivo sheep tissues (kidney, liver and spleen) were used to provide direct comparison of parameters. Finally, cavitation thresholds were evaluated for a subset of PVA samples with promising acoustic properties (attenuation, sound speed).

Identification of suitable formulation range

The manufacture of a FUS TMM imposes limitations on the gel formulation, as the polymer solution viscosity must avoid the entrapment of air bubbles prior to gelation and also support the homogeneous distribution of added scatterers throughout the manufacturing process. This restricted the maximum concentration of polymer (both PVA and cellulose) and determined the most suitable PVA molecular weight range, as summarized below. The molecular weight of PVA strongly influences its water solubility and the gelation process (Xue et al. 2015). In contrast to medium- and high-molecular-weight PVA gels, which withstood 20°C−45°C temperature increases during acoustic characterization without melting, low-molecular-weight PVA gels (31,000−50,000 g/mol) were mechanically unstable for temperatures above RT (see Fig. 3). However, high-molecular-weight PVA (146,000−186,000 g/mol) took longer to dissolve, and the higher viscosity of the solution increased the risk of air bubble entrapment during manufacture. As its acoustic properties remained comparable to those of gels prepared from 85,000−124,000 g/mol PVA_{medium}, the latter appeared best suited for this work, particularly at concentrations between 10% and 15%. Increasing the PVA concentration up to 20% was challenging, although possible, but this may be considered close to the maximum PVA concentration achievable for FUS TMMs. Within the range investigated (≤10%), cellulose concentration did not appear to adversely affect polymer solution viscosity and hence it may be possible to increase cellulose content in 10% or 15% PVA_{medium} gels beyond this.

Acoustic properties

The acoustic properties of PVA hydrogels (sound speed and attenuation coefficient, including its frequency dependence) were investigated as a function of PVA molecular weight and concentration and cellulose scatterer concentration, at temperatures between 20°C and 45°C. The attenuation of the PVA_{medium} gels was determined mainly by the concentration of cellulose (slope: 0.028 ± 0.012 dB/cm·MHz), whereas PVA concentration had a stronger influence on sound speed, yielding only a moderate increase (slope: 0.005 ± 0.003 dB/cm·MHz) in attenuation. Manufacture of gels with a higher cellulose concentration (>10%) or other scatterer (*e.g.,* glass beads, talcum powder or graphite; see Limitations and Outlook for PVA Phantom Use) may further increase attenuation to mimic higher-attenuation tissues. Overall, attenuation characteristics remained stable within the temperature range studied (20°C−45°C) while the speed of sound, as expected for a high water-content material, increased with temperature. The increase in sound speed in 10% PVA gels (slope: 1.35 ± 0.91 m/s) was less than the increase seen in pure water (slope: 1.99 ± 0.75 m/s). As sound speed decreases with temperature in fatty tissue (Bamber and Hill 1979), PVA hydrogels would be unsuitable for mimicking thermal exposure in such tissues. The acoustic properties of PVA cellulose gels meet the soft tissue properties criteria proposed by the International Electrotechnical Commission (IEC 2001) (sound speed = 1540 ± 15 m/s, attenuation coefficient = 0.5 ± 0.05 dB/cm at frequencies <10 MHz). The acoustic properties of human soft tissue are outlined in Table 4. The sound speed of 5%−20% PVA_{medium} gels fell within their range at temperatures of 35°C and 40°C. While the attenuation coefficients of gels with high PVA concentration and/or added cellulose was similar to those of human liver and spleen, the values of all PVA gels investigated were lower than those quoted for human kidney, brain and muscle. Given the relatively high attenuation coefficient (1.095 dB/cm at 1 MHz) of muscle, it is unlikely this can be matched using PVA cellulose gels; however, brain or kidney TMMs could be achieved by using >10% cellulose. Acoustic property differences between tissues are likely because of varying proportions of fat, parenchyma and blood. Within the range of uncertainties in this study, all acoustic properties of ex vivo sheep kidney and spleen were matched by the range of PVA gel formulations evaluated. Liver has a higher collagen content than the other tissues, and may also be more inhomogeneous. For example, it contains larger blood vessels. Whereas the sound speed and frequency dependence of ex vivo sheep liver fell within the range of values measured in PVA hydrogels, the attenuation coefficient of this tissue exceeded the maximum achievable, here in a 10% PVA 10% cellulose composite

Table 4. Sound speed, attenuation coefficient, thermal conductivity and specific heat capacity for selected human soft tissues and tissue-mimicking materials taken from the literature and in context with the measurements presented

Tissue	Temperature (°C)	Sound speed (m/s)	Attenuation at 1 MHz (dB/cm/MHz)	N	Thermal conductivity (W/mK)	Specific heat capacity ($MJ/m^3/K$)	Reference
Brain	22−37	1560	0.435−0.6		0.51 ± 0.02	3.63 ± 0.07	Cafarelli et al. 2017
Fat	35−37	1479	0.48		0.21 ± 0.02	2.35 ± 0.37	Duck 1990
Kidney	RT	1545 ± 7.8	0.38 ± 0.23	1.3 ± 0.26	0.51 ± 0.01	3.73 ± 0.61	Own measurement
Kidney	37	1560 ± 1.8	0.85		0.54 ± 0.04	3.74 ± 0.21	Duck 1990
Liver	RT	1563 ± 9.5	0.53 ± 0.14	1.14 ± 0.17	0.49 ± 0.07	3.07 ± 0.77	Own measurement
Liver	37	1560 ± 20.5	0.53 ± 0.24		0.5 ± 0.04	3.6	Duck 1990
Muscle	18−37	1547	1.1		0.49 ± 0.04	3.42 ± 0.46	Cafarelli et al. 2017
Spleen	RT	1607 ± 2.1	0.4 ± 0.24	1.29 ± 0.12			Own measurement
Spleen	37	1560 ± 10	0.43 ± 0.07		0.26	3.72	Duck 1990
10% PVA	RT	1556 ± 26	0.09 ± 0.02	1.43 ± 0.21	0.6 ± 0.02	3.14 ± 0.07	Own measurement
10% PVA 5% cellulose	RT	1552 ± 16	0.27 ± 0.04	1.3 ± 0.11	0.57 ± 0.01	3.19 ± 0.22	Own measurement
10% PVA 10% cellulose	RT	1563 ± 16	0.37 ± 0.02	1.31 ± 0.04	0.61 ± 0.02	2.7 ± 0.27	Own measurement
15% PVA	RT	1577 ± 9	0.13 ± 0.01	1.33 ± 0.09	0.58 ± 0.01	3.29 ± 0.23	Own measurement
20% PVA	RT	1590 ± 19	0.14 ± 0.02	1.43 ± 0.08	0.57 ± 0.02	3.34 ± 0.15	Own measurement

PVA = poly(vinyl alcohol); RT = room temperature.

gel. Given the linear relationship of attenuation coefficient with cellulose content, it is expected that by increasing this content, liver tissue could also be mimicked more closely.

Compared with previously published PVA-gel TMM formulations, Holt and Roy (2001) achieved a lower sound speed than the 5% PVA gel analyzed here (molecular weight, number of freeze thaw cycles not stated) and much higher attenuation coefficient at 1 MHz (0.63 ± 0.05 dB/cm). They produced a gel of low PVA polymer concentration (4% PVA) with addition of graphite powder for scattering and 1-propanol to reduce the gel's sound speed. A sound speed reduction through addition of 7% (v/v) 1-propanol was, however, not seen in PVA gels with or without cellulose in a preliminary study here (Fig. S3, online only). Additionally, our 5% PVA gels exhibited visible scatterer sedimentation, which was not reported by Holt and Roy (2001) for their gels. It may be that differences in (unreported) crosslinking procedures and PVA molecular weight may explain these discrepancies.

Kharine et al. (2003) and Zell et al. (2007) produced gels of 20% PVA (85,000−140,000 g/mol and 145,000 g/mol) using one 24-h freeze-thaw cycle, and added dimethylsulfoxide (DSMO) to create transparent gels. At RT, the sound speeds for these gels were comparable (1570−1590 m/s) to our results.

Both studies reported lower values for the attenuation coefficient than were measured here for 20% PVA gels. This may be attributed to fewer freeze-thaw cycles, as well to the addition of DSMO. Adding DSMO is attractive for the creation of transparent gels, achieved by lowering the PVA solution's freezing point. However, alterations in the freeze-thaw process may change the crystallization process, creating larger crystals with more space between them (Hassan and Peppas 2000). The addition of scatterers could mitigate the attenuation loss but may decrease gel transparency. Different types of scatterers could be incorporated to further optimize the gel's attenuation and sound speed. Taghizadeh et al. (2018) created a 10% PVA gel using two freeze-thaw cycles with an attenuation coefficient of 0.16 ± 0.01 dB/cm and sound speed of 1520 ± 10 m/s. They investigated increasing attenuation by adding graphite powder and talc powder. Although adding graphite powder created an inhomogeneous gel, addition of 10 g of talcum powder to a 250 mL PVA solution significantly increased attenuation to 0.89 dB/cm·MHz, higher than measured in this work, while sound speed was unaltered. Hence, talcum powder may be a suitable alternative to cellulose where higher attenuation is desirable.

Cavitation thresholds

Cavitation thresholds depend on how they are defined and the detection techniques used, as well as the frequency, exposure (pulse) duration, pressure amplitude and material exposed, the latter two aspects having been investigated in this study. At 1.66 MHz, for 10 ms duration pulses, all PVA cellulose hydrogels investigated using our 19-mm-diameter polyvinyl difluoride sensor with notch filtering of the drive signal and −20 dB signal amplification revealed a typical sigmoidal dependence of inertial cavitation probability on PNP. As the 0% and 100% cavitation thresholds are approached asymptotically, we determined the 25%, 50% and 75% thresholds (Table 3). However, other threshold levels can be obtained from the graphical results presented (Fig. 6). In 10% PVA gels, the 50% inertial cavitation detection threshold (*i.e.,* half of the ten 10 ms pulses delivered to

each position in the gel) lay in a cellulose content-dependent range of 3.5 MPa (10% cellulose) to 4.6 MPa (0% cellulose) (Table 3). Cellulose decreased this threshold, by up to 1 MPa, presumably as a result of the introduction of additional nucleation sites. Cavitation thresholds strongly depend on the specific insonation parameters. We suggest that PVA phantoms are best suited to applications involving the absorption of ultrasound, specifically HIFU (as long as the melting point of the gel is avoided) and hyperthermia (*i.e.,* longer-duration exposures with temperatures typically up to 45˚C). To judge the application of PVA for histotripsy, the mechanical properties (*e.g.,* elasticity, viscosity and stiffness) of the gels are important, and therefore, future mechanical characterization of PVA cryogels is a high priority. We plan to further investigate the elastic properties along with the intrinsic and shock-wave histotripsy thresholds for this phantom. For intrinsic histotripsy, short (1 cycle) pulses at higher pressures (25 MPa PNP) are typically required, whereas our pulses were 10 ms (10 cycles) long. While it would be possible to analyze the first cycle (or first few cycles) independently to investigate intrinsic histotripsy cavitation thresholds, this was not the intention of the study and the transducer used is not intended for this. The presented data, measured in the context of longer exposures, are, however, relevant to boiling histotripsy-type exposures and shed some further light on drug delivery and thermal ablation by giving the threshold for the phantom in the absence of introduced microbubbles and additional heating, respectively. These measurements will help to identify where cavitation should be expected and therefore aid study design for boiling histotripsy, drug delivery and thermal ablation. Given our lack of relevant cavitation threshold measurements in tissue, because of the limited samples, we provide an in-depth comparison with previously reported literature on this topic:

Cavitation thresholds have previously been measured in agar, agarose and gelatine hydrogels. Paris et al. (2018) created a vessel phantom consisting of 1.25% (w/v) agarose, to mimic tumor tissue. Defining the cavitation threshold as the appearance of a broadband signal 10 times higher than the background noise, they detected cavitation from 0.6 MPa, and found the 70% threshold to be at 2 MPa for their 0.5 MHz transducer. At 1.6 MHz, cavitation was first detected at 1.5 MPa, and the 70% threshold was reached at 4.3 MPa. This is similar to the 75% cavitation threshold of 4 MPa (Table 3) measured here at 1.66 MHz for PVA with 10% cellulose. Haller et al. (2018) and Haller and Wilkens (2018) investigated the 50% cavitation thresholds for agar-based phantoms for both continuous and burst sonications. The values measured in this work consisted of ten 10 ms burst pulses, thus making them more comparable to their measurements for 25-cycle burst length (10 ms burst period). The 50% cavitation threshold for PVA gels without cellulose (3.45 ± 0.18 MPa) is lower than the 4.6 MPa reported by Haller and Wilkens (2018). Cavitation thresholds (in terms of exposure) are expected to be lower, as Haller et al. (2018) quoted their 50% cavitation threshold for agar-based materials at 0.58 ± 0.12 MPa for a 3 ms continuous wave, and Bull et al. (2013) quoted 100% cavitation thresholds at 1.7 MHz for 3 s exposures in agar at 0.45 ± 0.07 MPa. We therefore conclude that PVA gels appear to cavitate less readily than agar gels subjected to longer exposure durations. In addition to measurements of cavitation thresholds in agar, Bull et al. (2013) reported the 100% threshold in ex vivo bovine liver at 2.62 ± 0.39 MPa. This is well below the 75% cavitation thresholds measured for all PVA (cellulose) gels in this work (4−6.5 MPa). As the cavitation thresholds in the PVA (cellulose) gels are driven by cellulose content, increasing the cellulose content could be used to achieve values similar to those of bovine liver.

However, the 50% threshold of our PVA gels was well below some previously reported threshold values for intrinsic histotripsy in soft tissue (pork atrial wall) and tissue phantoms (gelatine) (13.5−21 MPa) (Xu et al. 2007). Xu et al. (2007) investigated up to 200 pulses (<20 μs) at 750 kHz, but used high-speed imaging to detect bubble clouds, which are seen at higher PNPs than when a PCD is used. Maxwell et al. (2013) reported even higher values (26−30 MPa) for the 50% cavitation threshold in gelatine at 1.1 MHz (single, 0.44-2.86 μs pulse), using a PCD with a high-bandwidth 5 MHz focused transducer (with focal length of 10 cm). Within the PNP range assessed (1.8−9.6 MPa), cavitation detection remained below 25% in deionized degassed water. This does not contradict previous results (Maxwell et al. [2013], 50% threshold >17.7 MPa). However, it should be noted that differences in cavitation threshold pressure levels will arise depending on how "cavitation threshold" is defined and measured. While our cavitation thresholds were defined based on the fraction of pulses for which bubble activity was detected, Maxwell et al. (2013) reported cavitation probability of 50% for a single, short (microsecond length, 0.44−2.86 μs), focused pulse at 1.1 MHz. Therefore, when comparing cavitation thresholds, their definition must be kept in mind.

Thermal properties

Because of limitations in the availability of fresh sheep tissue, in particular the spleen, measurements of acoustic properties were here prioritized over thermal characterization and cavitation thresholds. We attempted

to address this limitation by thorough comparison with literature data. The thermal properties of the PVA formulations studied were in a range similar to, but not overlapping, that of soft tissue (Fig. 8D, 8E) and depended on PVA concentration with no significant dependence on cellulose concentration. The PVA gel formulations tested had a specific heat capacity that was lower than the range of human soft tissue (Table 4), with PVA concentrations from 10%−20% coming closest. Similarly, the thermal conductivity of the PVA gels was higher (10% PVA 5% cellulose: 0.57 ± 0.01 W/m·K) than the values found in Duck (1990), liver (0.5 ± 0.04 W/m·K) and spleen (0.26 W/m·K), although the kidney data (0.54 ± 0.04 W/m·K) overlapped with the quoted values. The thermal properties of PVA gels were all higher than those of fat (Table 4). As such, PVA hydrogels could be considered to be close to the range (PVA thermal conductivity 10%−12%, excluding spleen, specific heat capacity in the range) of human soft tissue in terms of their thermal properties, but these differences should be taken into account if using these TMMs for thermal FUS experiments used to determine exposure conditions in humans or for comparison with simulations.

Limitations and outlook for PVA phantom use

Despite providing a relatively comprehensive analysis of PVA gel characteristics as a function of PVA and cellulose concentration, and of PVA molecular weight and temperature dependence of sound speed and attenuation, there are several aspects of PVA-based TMMs that were not addressed in this study. These include the method of PVA crosslinking, the production of non-transparent samples, the evaluation of different scatterers, in addition to the current lack of long-term stability studies. The properties of PVA hydrogels depend on the specific method of crosslinking (Hassan and Peppas 2000). Here, only physical crosslinking using a fixed freeze-thawing process was investigated. This provided a reproducible, non-toxic procedure. The specific freezing and thawing gradients induced, the freeze-thaw cycle duration and number, and the gel-containing vessel (volume and thermal properties) may further influence the final gel properties. Here only relatively thin (0.6−1.2 cm) sheets of PVA hydrogel were produced, for which 5 h was sufficient to freeze the sample fully and 19 h to completely defrost it. Further investigation would be required to quantify the impact of differences in the freeze-thaw process on gel properties. A second limitation of the PVA TMMs investigated is the lack of optical transparency provided by freeze-thaw crosslinking. This prevents high-speed camera studies of acoustic cavitation activity, such as jetting. Changing the crosslinking procedure, for example, to the use of ionizing radiation exposure (Yang et al. 2007) or by the addition of DMSO improves transparency. However, the potential for creation of bigger crystallites (Hassan and Peppas 2000) is likely to affect the gel's mechanical stability, affecting cavitation thresholds and attenuation. Careful consideration of the most important properties of a TMM for a specific application and adjustment of gel formulations and crosslinking procedures accordingly are recommended.

The type of added scatterer is another aspect that requires further investigation as our analysis was limited to the use of cellulose. Talcum powder (Taghizadeh et al. 2018), graphite or glass beads may be suitable alternatives that, at low concentration, could boost attenuation, but may also affect cavitation thresholds. We consider the present study a sufficiently comprehensive starting point to motivate further investigation within the community for their specific needs.

An important point requiring future investigation is the (long-term) stability of the samples as only 1- to 3-day-old samples were investigated here. Given the formulation of a composite rather than a crosslinked PVA−cellulose gel, it remains questionable whether the cellulose content could be maintained during long-term storage. A further challenge regarding sample storage relates to sample contamination (*e.g.,* bacterial/fungal growth), degassing and water content.

Overall, PVA−cellulose hydrogels provide acoustic, cavitation and thermal properties sufficiently close to, or within the range of, those of soft tissue, and are relatively easily tunable to mimic different tissues. For FUS experiments, it is beneficial that the PVA (cellulose) gels can be heated to at least 45°C, are mechanically stable, have reproducible properties and are inexpensive and non-toxic. Their cavitation thresholds also make them attractive as a TMM for use in absorbing ultrasound, creating heating for hyperthermia or ablation without cavitation for cell exposure (Brüningk et al., 2019). As PVA cryogels, especially without added scatterers, do not appear to cavitate readily, they could be used as mimics for US drug delivery or boiling histotripsy, as well as for the testing of bubble formation in soft materials and, as they have been extensively characterized, to validate simulations. In comparison to other TMMs (*e.g.,* agar and gelatine gels that are relatively fragile), PVA forms more robust, high-melting-point gels (similar to polyacrylamide, but without the use of neurotoxic ingredients). Although PVA gel has to be heated during manufacture (like agar and gelatine), it does not form a solid gel on cooling, thus allowing other ingredients to be added prior to gelation, for example, thermochromic dyes Ambrogio et al. (2020). This also offers greater future potential for use in histotripsy applications.

CONCLUSIONS

Poly(vinyl alcohol) hydrogel manufacture using three freeze-thaw cycles produced properties that were reproducible, and the acoustic attenuation and sound speed were stable over a temperature range of 20˚C to 45˚C. Gels comprising 10%−15% 85,000−124,000 g/mol PVA provide an ideal base formulation with tunable acoustic and cavitation properties through the addition of scatterers, such as cellulose. The gel acoustic and thermal properties lie within the previously published ranges for human tissue and match those measured for sheep tissue in this study. PVA composite hydrogels could hence be custom designed to mimic a range of soft tissues with further room for improvement of the attenuation and optical properties. As such we recommend PVA hydrogels as suitable TMMs for soft tissues in both thermal and mechanical applications of therapeutic ultrasound.

Acknowledgments—This project has received funding from the European Union Horizon 2020 research and innovation program under Marie Skodowska-Curie Grant Agreement No. 813766.

SUPPLEMENTARY MATERIALS

Supplementary material associated with this article can be found in the online version at doi:10.1016/j.ultrasmedbio.2022.02.007.

REFERENCES

Ambrogio S, Basso RdM, Gomis A, Rivens I, Haar Gt, Zeqiri B, Ramnarine KV, Fedele F, Miloro P. A polyvinyl alcohol-based thermochromic material for ultrasound therapy phantoms. Ultrasound Med Biol 2020;46:3135–3144.

Apfel RE. Acoustic cavitation. Methods in experimental physics. 19Ultrasonics. Amsterdam: Elsevier; 1981. p. 355–411.

Bamber J, Hill C. Ultrasonic attenuation and propagation speed in mammalian tissues as a function of temperature. Ultrasound Med Biol 1979;5:149–157.

Brüningk SC, Rivens I, Mouratidis P, ter Haar G. Focused ultrasound mediated hyperthermia in vitro: An experimental arrangement for treating cells under tissue-mimicking conditions. Ultrasound Med Biol 2019;45:3290–3297.

Bull V, Civale J, Rivens I, ter Haar G. A comparison of acoustic cavitation detection thresholds measured with piezo-electric and fiber-optic hydrophone sensors. Ultrasound Med Biol 2013;39:2406–2421.

Cabrelli LC, Pelissari PI, Deana AM, Carneiro AA, Pavan TZ. Stable phantom materials for ultrasound and optical imaging. Phys Med Biol 2017;62:432–447.

Cafarelli A, Verbeni A, Poliziani A, Dario P, Menciassi A, Ricotti L. Tuning acoustic and mechanical properties of materials for ultrasound phantoms and smart substrates for cell cultures. Acta Biomater 2017;49:368–378.

Coakley WT, Nyborg W. Cavitation: Dynamics of gas bubbles in ultrasound. In: Fry FJ, (ed). Ultrasound: Its applications in medicine and biology. Amsterdam/New York: Elsevier; 1978. p. 77–159.

Cook JR, Bouchard RR, Emelianov SY. Tissue-mimicking phantoms for photoacoustic and ultrasonic imaging. Biomed Opt Express 2011;2:3193–3206.

Crivoi F, Stefan L, Moldovan L, Vasile C. Compatibility and cytotoxicity testing of some polyvinyl alcohol and hydrolyzated collagen based blends. Romanian Biotechnol Lett 2007;12:3495–3503.

Culjat MO, Goldenberg D, Tewari P, Singh RS. A review of tissue substitutes for ultrasound imaging. Ultrasound Med Biol 2010;36:861–873.

Duck FA. Physical properties of tissue: A comprehensive reference book. London: Academic Press; 1990.

Gustavsson M, Karawacki E, Gustafsson SE. Thermal conductivity, thermal diffusivity, and specific heat of thin samples from transient measurements with hot disk sensors. Rev Sci Instrum 1994;65:3856–3859.

Haller J, Wilkens V. Determination of acoustic cavitation probabilities and thresholds using a single focusing transducer to induce and detect acoustic cavitation events: II. Systematic investigation in an agar material. Ultrasound Med Biol 2018;44:397–415.

Haller J, Wilkens V, Shaw A. Determination of acoustic cavitation probabilities and thresholds using a single focusing transducer to induce and detect acoustic cavitation events: I. Method and terminology. Ultrasound Med Biol 2018;44:377–396.

Hassan CM, Peppas NA. Structure and applications of poly(vinyl alcohol) hydrogels produced by conventional crosslinking or by freezing/thawing methods. In: Waldmann H, (ed). Biopolymers · PVA hydrogels, anionic polymerisation nanocomposites. Advances in polymer science, Vol. 153. Berlin/Heidelberg: Springer; 2000. p. 37–65.

Hill CR, (ed). Physical principles of medical ultrasonics. 2nd edition-Chichester: Wiley; 2004.

Holt RG, Roy RA. Measurements of bubble-enhanced heating from focused, MHz-frequency ultrasound in a tissue-mimicking material. Ultrasound Med Biol 2001;27:1399–1412.

Hou Y, Chen C, Liu K, Tu Y, Zhang L, Li Y. Preparation of PVA hydrogel with high-transparence and investigations of its transparent mechanism. RSC Adv 2015;5:24023–24030.

Howard S, Yuen J, Wegner P, Zanelli CI. Characterization and FEA simulation for a HIFU phantom material. Proc IEEE Int Symp Ultrason 2003;2:1270–1273.

Hu Y, Wan JM, Yu AC. Membrane perforation and recovery dynamics in microbubble-mediated sonoporation. Ultrasound Med Biol 2013;39:2393–2405.

Kharine A, Manohar S, Seeton R, Kolkman RG, Bolt RA, Steenbergen W, de Mul FF. Poly(vinyl alcohol) gels for use as tissue phantoms in photoacoustic mammography. Phys Med Biol 2003;48:357–370.

Lafon C, Zderic V, Noble ML, Yuen JC, Kaczkowski PJ, Sapozhnikov OA, Chavrier F, Crum LA, Vaezy S. Gel phantom for use in high-intensity focused ultrasound dosimetry. Ultrasound Med Biol 2005;31:1383–1389.

Lee JH, Lee US, Jeong KU, Seo YA, Park SJ, Kim HY. Preparation and characterization of poly(vinyl alcohol) nanofiber mats cross-linked with blocked isocyanate prepolymer: Crosslinked PVA/BIP nanofiber mats. Polym Int 2010;59:1683–1689.

Maolin Z, Yoshii F, Kume T, Hashim K. Syntheses of PVA/starch grafted hydrogels by irradiation. Carbohydr Polym 2002;50:295–303.

Maxwell AD, Cain CA, Hall TL, Fowlkes JB, Xu Z. Probability of cavitation for single ultrasound pulses applied to tissues and tissue-mimicking. Ultrasound Med Biol 2013;39:449–465.

Miller DL, Smith NB, Bailey MR, Czarnota GJ, Hynynen K, Makin I. American Institute of Ultrasound in Medicine Bioeffects Committee. Overview of therapeutic ultrasound applications and safety considerations. Ultrasound Med Biol 2013;39:449–465.

Miller NL, Lingeman JE. Management of kidney stones. Br Med J 2007;334:468–472.

Paris JL, Mannaris C, Cabaas MV, Carlisle R, Manzano M, Vallet-Reg M, Coussios CC. Ultrasound-mediated cavitation-enhanced extravasation of mesoporous silica nanoparticles for controlled-release drug delivery. Chem Eng J 2018;340:2–8.

Prokop AF, Vaezy S, Noble ML, Kaczkowski PJ, Martin RW, Crum LA. Polyacrylamide gel as an acoustic coupling medium for focused ultrasound therapy. Ultrasound Med Biol 2003;29:1351–1358.

Retat L. Characterization of the acoustic, thermal and histological properties of tissue required for high intensity focused ultrasound (HIFU) treatment planning. PhD thesis. : Institute of Cancer Research, University of London; 2011.

Roberts WW. Development and translation of histotripsy: Current status and future directions. Curr Opin Urol 2014;24:104–110.

Silver F, Shah R. Measurement of mechanical properties of natural and engineered implants. Adv Tissue Eng Regen Med Open Access 2016;1:20–25.

Taghizadeh S, Labuda C, Mobley J. Development of a tissue-mimicking phantom of the brain for ultrasonic studies. Ultrasound Med Biol 2018;44:2813–2820.

ter Haar G. Therapeutic applications of ultrasound. Prog Biophys Mol Biol 2007;93:111–129.

ter Haar G, Coussios C. High Intensity Focused Ultrasound: Past, present and future. Int J Hyperthermia 2007;23:85–87.

Unger EC, Matsunaga TO, McCreery T, Schumann P, Sweitzer R, Quigley R. Therapeutic applications of microbubbles. Eur J Radiol 2002;42:160–168.

Vlaisavljevich E, Greve J, Cheng X, Ives K, Shi J, Jin L, Arvidson A, Hall T, Welling TH, Owens G, Roberts W, Xu Z. Non-invasive ultrasound liver ablation using histotripsy: Chronic study in an in vivo rodent model. Ultrasound Med Biol 2016;42:1890–1902.

Xu Z, Raghavan M, Hall T, Chang CW, Mycek MA, Fowlkes J, Cain C. High speed imaging of bubble clouds generated in pulsed ultrasound cavitational therapy—Histotripsy. IEEE Trans Ultrason Ferroelectr Freq Control 2007;54:2091–2101.

Xue R, Xin X, Wang L, Shen J, Ji F, Li W, Jia C, Xu G. A systematic study of the effect of molecular weights of polyvinyl alcohol on polyvinyl alcohol graphene oxide composite hydrogels. Phys Chem Chem Phys 2015;17:5431–5440.

Yang X, Liu Q, Chen X, Yu F, Zhu Z. Investigation of PVA/ws-chitosan hydrogels prepared by combined 7-irradiation and freeze-thawing. Carbohydr Polym 2007;73:401–408.

Yang L, Zhang HY, Yang Q, Dn Lu. Bacterial cellulose-poly(vinyl alcohol) nanocomposite hydrogels prepared by chemical crosslinking. J Appl Polym Sci 2012;126:E245–E251.

Yang C, Li Y, Du M, Chen Z. Recent advances in ultrasound-triggered therapy. J Drug Target 2019;27:33–50.

Zell K, Sperl JI, Vogel MW, Niessner R, Haisch C. Acoustical properties of selected tissue phantom materials for ultrasound imaging. Phys Med Biol 2007;52:N475–N484.

Zhu L, Altman MB, Laszlo A, Straube W, Zoberi I, Hallahan DE, Chen H. Ultrasound hyperthermia technology for radiosensitization. Ultrasound Med Biol 2019;45:1025–1043.